Proceedings of the 11th World Congress on Electrical Engineering and Computer Systems and Sciences (EECSS'25)
Paris, France – August, 2025
Paper No. ICBES 177
DOI: 10.11159/icbes25.177

Automated Risk Stratification of Peripheral Artery Disease via Optimized Volume Rendering and Vascular Biomarkers

Mohammed A. AboArab[1,2], Vassiliki T. Potsika[1], Alexis Theodorou[3], Sylvia Vagena[3], Fragiska Sigala[3], and Dimitrios I. Fotiadis[1,4]

[1]Unit of Medical Technology and Intelligent Information Systems, Dept. of Materials Science and Engineering, University of Ioannina
Ioannina, GR45110, Greece
[2]Electronics and Electrical Communication Engineering Department, Faculty of Engineering, Tanta University
Tanta, Egypt
m.aboarab@uoi.gr; vpotsika@uoi.gr
[3]First Propaedeutic Dept. of Surgery, National and Kapodistrian University of Athens
Athens, Greece
alexiostheodorou@gmail.com; sylvievagena@med.uoa.gr; fsigala@med.uoa.gr
[4]Biomedical Research Institute, Foundation for Research and Technology-Hellas, University Campus of Ioannina
Ioannina, GR45110, Greece
fotiadis@uoi.gr

Abstract **-** Peripheral artery disease (PAD) is a progressive vascular condition requiring precise diagnostic tools for effective risk stratification. This study presents a novel computational framework that leverages optimized volume rendering, dynamic illumination, and quantitative vascular analysis to enhance the evaluation of PAD. The proposed system integrates real-time plaque density and vascular curvature assessments, providing noninvasive, efficient, and accurate diagnostics. The framework offers automated clinical decision support, reducing interobserver variability and improving diagnostic workflows. Initial validation demonstrated its ability to classify PAD risk effectively, with plaque density averaging 0.85 and vascular curvature averaging 1.3, correctly identifying high-risk cases within the tested cohort. This framework represents a transformative approach to PAD diagnostics, supporting early intervention and personalized patient management.

Keywords**:** Peripheral artery disease (PAD); Dynamic illumination; Plaque density analysis; Risk stratification; Vascular curvature; Volume rendering

1. Introduction

Peripheral artery disease (PAD) is a chronic and progressive vascular condition characterized by narrowing or obstruction of peripheral arteries due to atherosclerotic plaque buildup. Although PAD affects more than 230 million individuals worldwide, it represents a significant global health challenge, increasing the risk of severe cardiovascular events and limb ischemia [1]. Despite its prevalence, early diagnosis remains elusive, particularly in asymptomatic patients or those with atypical presentations. The clinical delay in detection often leads to advanced disease stages, which are associated with substantial morbidity and reduced quality of life. Traditional diagnostic methods, such as the ankle–brachial index (ABI), duplex ultrasound, and computed tomography angiography (CTA), have long been the cornerstone of PAD assessment [2]. While these techniques provide valuable insights, they are fraught with limitations. ABIs and ultrasounds are operator dependent and often lack the sensitivity to detect early-stage disease. Advanced imaging modalities such as CTA and magnetic resonance angiography (MRA) offer superior visualization but are resource intensive and costly and expose patients to ionizing radiation or contrast agents. Moreover, the complexity of vascular geometries, such as calcified lesions, stenotic regions, and tortuous arteries, poses significant challenges for accurate diagnosis and risk stratification [3]. Recent advancements in computational imaging and machine learning have revealed transformative opportunities to address these limitations. Techniques such as optimized volume rendering, high-dynamic-range illumination [4], and GPU-accelerated visualization offer unprecedented capabilities in vascular imaging [5]. By enhancing spatial resolution, reducing artifacts

from calcifications, and enabling real-time data processing, these methods allow for a more nuanced evaluation of complex vascular geometries and plaque characteristics. In addition, emerging AI-driven algorithms have shown promise in automating the analysis of imaging biomarkers, further streamlining diagnostic workflows [6].

Our study introduces a novel computational framework that leverages optimized volume rendering and dynamic illumination to redefine PAD diagnostics. By integrating automated assessments of plaque density and vascular curvature, the proposed approach addresses key diagnostic challenges, including the accurate stratification of PAD risk. The system's noninvasive nature, coupled with its efficiency and precision, has the potential to significantly enhance clinical decision-making and patient outcomes. Through this work, we aim to bridge the existing gaps in PAD diagnostics by demonstrating the transformative role of advanced computational tools. The integration of real-time visualization with automated analysis not only advances PAD risk classification but also lays the foundation for personalized treatment strategies in vascular medicine.

2. Materials and Methods

2.1. Real-Time Dynamic Illumination

The proposed framework integrates an advanced real-time dynamic illumination model to enhance the visualization of vascular structures, especially in PAD diagnostics. This illumination approach uses Perlin noise to simulate the dynamic light direction and a damped harmonic oscillator to generate realistic variations in light intensity over time [7]. These dynamic lighting techniques improve depth perception, enhance the realism of vascular geometry, and enable a detailed visualization of intricate anatomical structures.

The dynamic behavior of the light is controlled through mathematical formulations that adapt in real time on the basis of user-defined parameters. The light direction is calculated using a frequency-controlled noise factor, ensuring smooth and natural transitions. This is vital for achieving enhanced realism in visualizing complex vascular geometries. On the other hand, the light intensity is modulated using a damped harmonic oscillator model to introduce natural decay and oscillatory effects [8]. Together, these techniques provide a highly realistic simulation of lighting, significantly improving the perception of depth and texture in medical imaging applications.

Dynamic Light Direction [9]: The light direction vector $L(t)$ is computed as:

$$L(t) = \begin{bmatrix} \sin(\omega t) + 0.2\,\eta(t) \\ \cos(\omega t) - 0.2\,\eta(t) \\ \sin(0.5\omega t) \end{bmatrix}, \tag{1}$$

where the noise factor $\eta(t)$ is defined as:

$$\eta(t) = \sin(\omega t) \cdot \cos(\omega t), \tag{2}$$

where ω is the light frequency, which is defined by the user input, and where t is the current time.

Dynamic Light Intensity: The light intensity $I(t)$ is modeled as:

$$I(t) = I_0 + A \cdot e^{-\beta t} \cdot \sin(\alpha t), \tag{3}$$

where I_0 is the base intensity, A is the amplitude of oscillation, β is the damping factor, and α is the angular frequency.

2.2. Plaque Density Analysis

To quantitatively assess the extent of plaque accumulation within peripheral arteries, a voxel-based plaque density analysis was conducted [10]. This method uses the intensity values derived from Hounsfield units (HUs) in computed tomography (CT) imaging to segment and classify vascular tissues, enabling a precise evaluation of plaque burden [11, 12]. The analysis hinges on defining specific HU thresholds to categorize voxels into calcified plaque, soft plaque, and vascular tissue regions.

Thresholding: The classification of voxels is guided by predefined HU ranges as follows:

$$\text{Vascular Tissue: } 45 \leq HU \leq 300, \tag{4}$$

$$\text{Calcified Plaque: } 130 \leq HU \leq 300, \tag{5}$$

$$\text{Soft Plaque: } 50 \leq HU < 130. \tag{6}$$

This thresholding mechanism ensures the accurate segregation of vascular elements, allowing for the extraction of biomarkers associated with arterial health and disease.

Plaque density calculation: The plaque density (ρ_p) is computed as the ratio of plaque voxels (both calcified and soft) to the total vascular voxels within the specified region of interest [13]. The formula for calculating plaque density is:

$$\rho_p = \frac{N_c + N_s}{N_v}, \tag{7}$$

where N_c is the number of calcified plaque voxels, N_s is the number of soft plaque voxels, and N_v is the total number of vascular tissue voxels.

This metric provides a quantitative measure of atherosclerotic plaque burden, offering critical insights into the severity and progression of PAD. By combining HU-based segmentation with this density calculation, the framework supports enhanced diagnostic precision and risk stratification.

2.3. Vascular Curvature Analysis

The analysis of vascular curvature is crucial for evaluating arterial deformation and identifying regions subjected to high morphological stress, which are significant indicators of disease severity and progression [14]. By extracting a sequence of centerline points P_{i-1}, P_i, and P_{i+1} from the arterial geometry, the local curvature at each point is calculated [15]. This approach provides a detailed quantification of the arterial structure, enabling the detection of irregularities and potential risk zones.

The curvature k_i at a specific centerline point P_i is determined by the angle between the vectors connecting consecutive centerline points [16]. It is expressed mathematically as:

$$k_i = arccos\left(\frac{\vec{v_1} \cdot \vec{v_2}}{\|\vec{v_1}\| \|\vec{v_2}\|}\right), \tag{8}$$

$$\vec{v_1} = P_i - P_{i-1}, \tag{9}$$

$$\vec{v_2} = P_{i+1} - P_i, \tag{10}$$

where $\vec{v_1}$ is a vector from the previous point to the current point, $\vec{v_2}$ is a vector from the current point to the next point, and $\|\vec{v_1}\|, \|\vec{v_2}\|$ are the magnitudes of vectors $\vec{v_1}$ and $\vec{v_2}$, respectively.

Average Curvature Calculation [17]: To evaluate the overall curvature along the vascular centerline, the average curvature $\bar{k}$ is computed as the mean of all individual curvature values:

$$\bar{k} = \frac{\sum_{i=1}^{N-1} k_i}{N-2}, \tag{11}$$

where N is the total number of centerline points.

This metric provides a comprehensive assessment of arterial shape irregularities, aiding in the identification of critical morphological changes associated with vascular diseases. By integrating curvature analysis into the diagnostic process, this method enhances the precision and reliability of disease characterization.

2.4. PAD Risk Classification

PAD risk classification integrates both plaque density and vascular curvature metrics [18], leveraging threshold-based decision-making to stratify patients into high- or low-risk categories. This approach ensures a systematic and quantifiable framework for early identification and intervention in patients susceptible to PAD.

The framework uses predefined thresholds: the plaque density threshold ($\rho_{p,threshold} = 0.3$) and the curvature threshold ($\bar{k}_{threshold} = 0.5$). The classification rule is mathematically expressed as:

$$Risk\ Level = \begin{cases} High\ Risk, if\ \rho_p > \rho_{p,threshold}\ or\ \bar{k} > \bar{k}_{threshold}, \\ Low\ Risk, otherwise. \end{cases} \tag{12}$$

where ρ_p represents the computed plaque density and $\bar{k}$ denotes the average vascular curvature.

This methodology provides an efficient and robust tool for PAD risk assessment, enabling clinicians to prioritize patients who may benefit from advanced diagnostic and therapeutic interventions. The threshold-based approach simplifies the integration of the algorithm into real-time diagnostic systems, thereby enhancing clinical decision-making processes.

2.5. Implementation Details

The proposed framework was implemented using vtk.js [19] for advanced volume rendering and WebAssembly [20] to ensure efficient computation and performance optimization. The integration of real-time dynamic illumination and automated analysis modules into a web-based platform guarantees both accessibility and scalability for clinical and research applications. The system processes CT imaging data in real time, enabling interactive exploration and detailed analysis of vascular structures.

2.6. Dataset Description

The dataset used in this study, provided by the National and Kapodistrian University of Athens, comprises CT scans from 22 patients diagnosed with PAD. Using a Revolution EVO CT scanner, the dataset features an average of 352 slices per patient and an average file size of 182 MB. All patients provided written informed consent for the use of their anonymized data in research. The data were anonymized and randomly selected from the hospital system for ethical compliance, with research protocol approvals under protocol numbers 9876/28.3.24 and 11293/9.4.24.

3. Results

3.1. Effect of Light Controls on CT DICOM Peripheral Artery Imaging

Dynamic light controls play a pivotal role in enhancing the visualization of CT DICOM images, particularly for the evaluation of PADs. Fig. 1 illustrates the impact of three critical parameters—light rotation speed, base intensity, and intensity amplitude—on the imaging quality and clinical interpretability of vascular structures. These parameters enable tailored visualization, facilitating the identification of arterial abnormalities and enhancing diagnostic accuracy. The user interface, as shown in Fig. 1(a), provides precise control over the lighting parameters. The light rotation speed, initially set to 0.001, governs the dynamic transitions of light over vascular surfaces, aiding in the identification of calcified plaques and soft tissue variations. The base intensity, with a default value of 0.5, modulates the ambient brightness, ensuring balanced contrast across the vascular and surrounding regions. The intensity amplitude, also set to 0.5 by default, introduces oscillatory variations in lighting, enhancing depth perception and emphasizing surface textures. Fig. 1(b) presents the full 3D CT volume of patient 9 under the default lighting parameters. This configuration achieves balanced illumination, enabling an overall assessment of the vascular geometry.

Focused visualization of the pelvic region is shown in Fig. 1(c), (d), and (e) under dynamic lighting with the default rotation speed (0.001), base intensity (0.5), and intensity amplitude (0.5). In Fig. 1(c), the rotational light highlights the arterial walls and surrounding tissues, aiding in the identification of subtle vascular deformities. Fig. 1(d) and Fig. 1(e) further enhance depth perception and contrast, improving differentiation between calcified plaques and soft tissues, which is essential for precise plaque characterization and arterial health assessment. In Fig. 1(f), the light rotation speed is slightly increased to 0.002, the base intensity is reduced to 0, and the intensity amplitude is set to 1. This setup enhances contrast resolution and accentuates vascular surface gradients, thereby delineating arterial wall morphology with better precision. Fig. 1(g) shows the maximum light rotation speed (0.01) and intensity amplitude (1), with the base intensity maintained at 0. Rapid light transitions accentuate surface textures and regions of high curvature, offering enhanced visualization of complex vascular deformations. However, rapid oscillations may introduce artifacts, potentially complicating the evaluation of smaller or less prominent features. Fig. 1(h) shows the effect of static lighting, which is achieved with a rotation speed of 0, a base

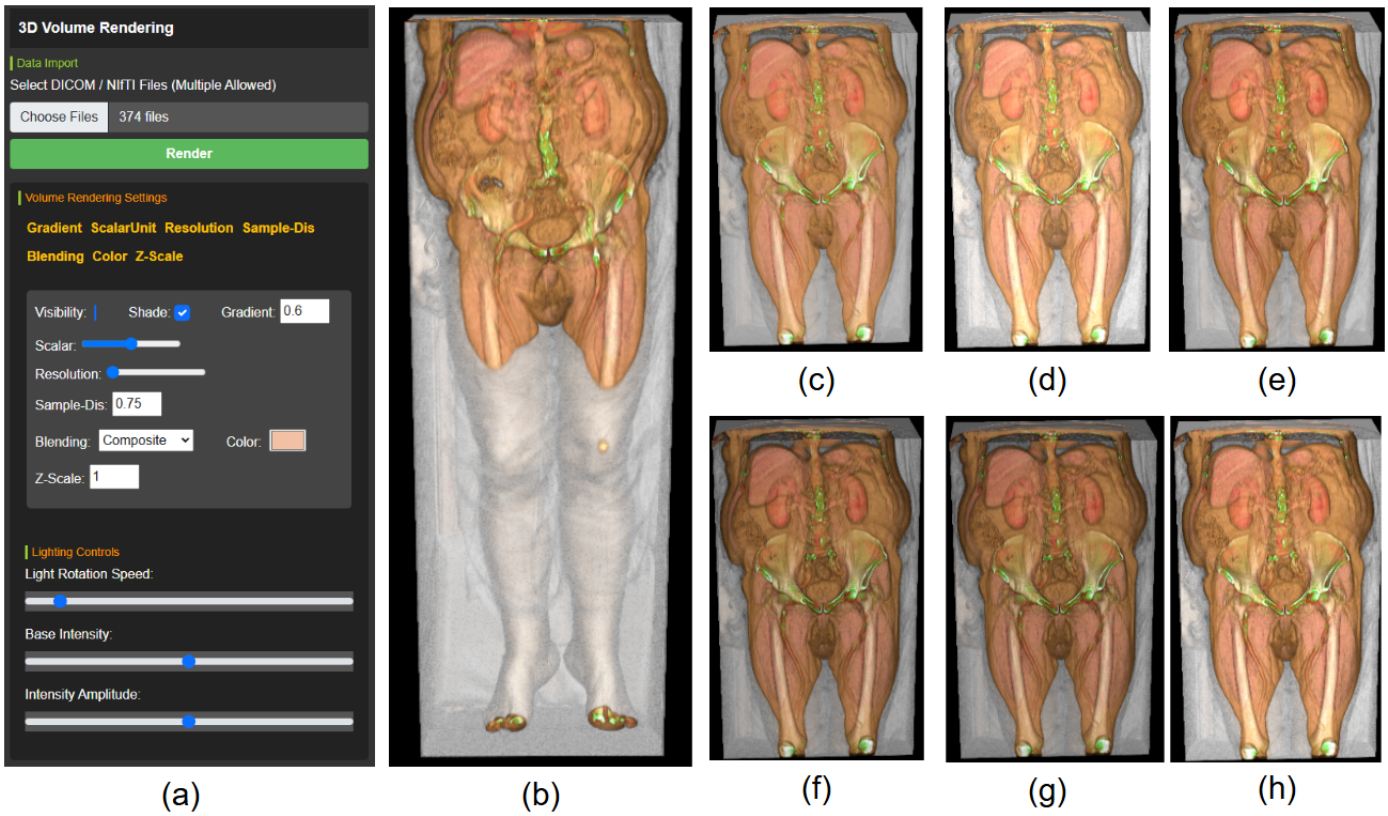

Fig. 1: Interactive Visualization of Peripheral Artery CT Imaging for Patient 9 with Dynamic Light Controls; (a) User interface for light control parameters; (b) Full CT volume visualization; (c-e) Region of interest under dynamic light variation; (f) Increased light rotation speed and maximum intensity amplitude; (g) Maximum light rotation speed and intensity amplitude; (h) Static lighting with medium intensity.

Table 1: Quantitative Results of Plaque Density and Vascular Curvature Metrics Across Patients.

Patient ID	Total Vascular Voxels	Calcified Plaque Voxels	Soft Plaque Voxels	Plaque Density	Total Centerline Points	Average Curvature	PAD Risk Classification
1	5534139	798390	3810908	0.8329	299684	1.132	High Risk
2	4853409	1178950	2975082	0.8559	218375	1.4366	High Risk
3	4551532	1155706	2952517	0.9026	234276	1.2712	High Risk
4	13067145	1463447	10616052	0.9244	234132	1.5417	High Risk
5	3499743	721625	2102619	0.807	255167	1.1786	High Risk

intensity of 0.5, and an intensity amplitude of 0.5. Uniform and stable lighting facilitates a detailed evaluation of the region of interest, supporting the analysis of arterial wall integrity, plaque distribution, and vascular morphology without distractions from dynamic transitions.

3.2. Validation of the Proposed Framework for PAD Risk Classification

The initial results of the proposed framework, as presented in Table 1, provide a detailed quantitative analysis of plaque density and vascular curvature metrics for five patients diagnosed with PAD. These metrics represent preliminary validation of the framework's ability to assess vascular abnormalities and classify PAD risk effectively.

The plaque density (ρ_p) values ranged from 0.807 for patient 5 to 0.924 for patient 4. Elevated plaque density values indicate significant arterial plaque accumulation, reflecting advanced disease stages. For example, patient 4, with the highest plaque density of 0.924, presented with severe arterial obstruction and pronounced disease progression. The analysis of vascular curvature revealed average curvature values $(\bar{k})$ ranging from 1.132 (patient 1) to 1.541 (patient 4). These values are calculated from the total centerline points, with the highest count of 299,684 observed in patient 1. Higher curvature values signify tortuous arterial paths, increasing hemodynamic stress and the risk of vascular complications. Patient 4, who displays both the highest curvature $(\bar{k} = 1.541)$ and plaque density $(\rho_p = 0.924)$, is indicative of an advanced disease state with substantial vascular irregularities.

All five patients were classified as being at high risk of PAD, according to the framework's thresholds for plaque density (> 0.3) and vascular curvature (> 0.5). These results demonstrate the framework's capacity to quantify critical vascular features and classify PAD severity effectively in its initial application.

4. Discussion

The proposed framework, which is part of DECODE-3DViz [21], is an open source solution designed for efficient WebGL-based high-fidelity visualization of large-scale medical images. It represents a significant advancement in the automated risk classification of PAD by integrating optimized volume rendering, dynamic illumination, and quantitative vascular analysis. The ability to automatically assess plaque density and vascular curvature provides clinicians with a powerful tool for the early detection and risk stratification of PAD, which is critical for timely intervention and improved patient outcomes. By offering a quantitative and objective assessment of vascular health, the proposed system enhances diagnostic accuracy and supports personalized treatment strategies, ultimately reducing the morbidity and mortality associated with PAD.

The proposed framework outperforms existing tools such as VolView [22] and Glance [23], which lack automated clinical decision-making capabilities. As summarized in Table 2, while VolView and Glance provide robust visualization and basic analysis features, they do not support automated plaque density calculation, vascular curvature analysis, or risk classification. In contrast, the proposed system integrates these advanced functionalities, enabling a comprehensive and automated evaluation of PAD severity. This automation reduces the reliance on manual interpretation, minimizes interobserver variability, and enhances the efficiency of diagnostic workflows. Furthermore, the dynamic illumination model in the proposed framework offers superior visualization of vascular structures, improving the identification of subtle abnormalities that are missed with traditional tools. Despite its advancements, the proposed framework has certain

Table 2: Comparative Feature Analysis of the Proposed PAD Framework Versus Existing Tools (VolView and Glance).

Feature / Capability	**Proposed Framework**	**VolView [22]**	**Glance [23]**
Volume Rendering	✓	✓	✓
Dynamic Illumination	✓	✗	✗
Real-Time Light Control	✓	✗	✗
Automated Plaque Density Analysis	✓	✗	✗
Automated Vascular Curvature Analysis	✓	✗	✗
PAD Risk Stratification	✓	✗	✗
Clinical Decision Support	✓	✗	✗
Large-Scale Visualization	✓	✗	✗

limitations. First, the accuracy of plaque density and curvature analysis depends on the quality of the input CT data, which may be affected by imaging artifacts or low resolution. Second, the framework currently relies on predefined thresholds for risk classification, which may not account for patient-specific variations in vascular anatomy and disease progression.

Future work will focus on addressing these limitations and further enhancing the framework's capabilities. AI-based segmentation techniques will be integrated to improve the accuracy of peripheral artery and centerline extraction, enabling more precise quantification of plaque burden and vascular geometry. In addition, a comprehensive clinical validation of the proposed framework through two cohort-based studies. First, a retrospective study on previously collected datasets with known disease progression will be conducted to evaluate the accuracy of the risk stratification in identifying patients who required treatment for severe PAD. Second, a prospective cohort study will be initiated to follow newly diagnosed patients over a period of five years, assessing the predictive capability of the framework in real-world clinical scenarios. These steps aim to establish robust clinical evidence supporting the diagnostic and prognostic utility of the system. Finally, the framework will be optimized for cloud-based deployment, enabling scalable and accessible usage in healthcare.

5. Conclusion

The proposed computational framework integrates optimized volume rendering, dynamic illumination, and quantitative vascular analysis to redefine PAD diagnostics. By automating the assessment of plaque density and vascular curvature, the system enhances diagnostic precision, reduces interobserver variability, and streamlines clinical workflows. Initial validation demonstrated its ability to classify PAD risk effectively, offering a robust, noninvasive solution for early intervention and personalized patient management. The study utilized real clinical data for validation, confirming the practical applicability of the framework. Future work will focus on expanding the dataset, incorporating multimodal imaging, and integrating AI-based segmentation techniques to enhance clinical accuracy and support personalized vascular assessments.

Acknowledgements

This work received funding from the European Union's Horizon 2020 research and innovation program under Marie Skłodowska-Curie grant agreement 956470 as part of the DECODE (Drug-coated balloon simulation and optimization system for the improved treatment of peripheral artery disease) project.

References

[1] P. A. R. Peri-Okonny, Gaëlle Callegari, Santiago Cleman, Jacob Vashist, Aseem Smolderen, Kim G Mena-Hurtado, Carlos, Annals of Vascular Surgery, "Prediction of Health Status in Patients Undergoing Lower Extremity Intervention for Claudication," vol. 110, pp. 314-322, 2025.

[2] S. A. v. B. Willems, Obrecht O Schepers, Abbey van Schaik, Jan van der Vorst, Joost R Hamming, Jaap F Brouwers, Jeroen JWM, Annals of Vascular Surgery, "A Diagnostic Comparison Study between Maximal Systolic Acceleration and Acceleration Time to Detect Peripheral Arterial Disease," vol. 111, pp. 203-211, 2025.

[3] J. D. M. Theodore A Abbott, Ehtisham Parikh, Sahil A Aboulhosn, Jamil Ashwath, Mahi L Baranowski, Bryan Bergersen, Lisa Chaudry, Hannah I, Cardiovascular Interventions, "2023 ACC/AHA/SCAI Advanced Training Statement on Interventional Cardiology (Coronary, Peripheral Vascular, and Structural Heart Interventions) A Report of the ACC Competency Management Committee," vol. 16, no. 10, pp. 1239-1291, 2023.

[4] J. S. S. Park, Jae Woong Cho, Nam Ik, Multimedia Tools Applications, "Generation of high dynamic range illumination from a single image for the enhancement of undesirably illuminated images," vol. 78, pp. 20263-20283, 2019.

[5] J. L. Cao, Kit-Yung Lee, Lik-Hang Liu, Xiaoli Hui, Pan Su, Xiang, ACM Computing Surveys, "Mobile augmented reality: User interfaces, frameworks, and intelligence," vol. 55, no. 9, pp. 1-36, 2023.

[6] F. B. Lareyre, Christian-Alexander Chaudhuri, Arindam Lee, Regent Carrier, Marion Adam, Cédric Lê, Cong Duy Raffort, Juliette, Journal of vascular surgery, "Applications of artificial intelligence for patients with peripheral artery disease," vol. 77, no. 2, pp. 650-658. e1, 2023.

[7] P. S. Gómez, Marion Schützenberger, Anne Bohr, Christopher Döllinger, Michael, Medical biological engineering computing, "Low-light image enhancement of high-speed endoscopic videos using a convolutional neural network," vol. 57, pp. 1451-1463, 2019.
[8] Z. M. Li, Nosang Vincent Yin, Yadong, Science Robotics, "Light-powered soft steam engines for self-adaptive oscillation and biomimetic swimming," vol. 6, no. 61, p. eabi4523, 2021.
[9] P.-P. K. Sloan, Jan Snyder, John, "Precomputed radiance transfer for real-time rendering in dynamic, low-frequency lighting environments," in *Seminal Graphics Papers: Pushing the Boundaries, Volume 2*, 2023, pp. 339-348.
[10] L. A. Saba, Pier Luigi Gupta, Ajay Cau, Riccardo Paraskevas, Kosmas I Poredos, Pavel Wasserman, Bruce A Kamel, Hooman Avgerinos, Efthymios D Salgado, Rodrigo, Atherosclerosis, "International Union of Angiology (IUA) consensus paper on imaging strategies in atherosclerotic carotid artery imaging: From basic strategies to advanced approaches," vol. 354, pp. 23-40, 2022.
[11] A. J. G. J. Buckler, Antonio M Rajeev, Akshay Nicolaou, Anna Sakamoto, Atsushi St Pierre, Samantha Phillips, Matthew Virmani, Renu Villines, Todd C, Atherosclerosis, "Atherosclerosis risk classification with computed tomography angiography: a radiologic-pathologic validation study," vol. 366, pp. 42-48, 2023.
[12] H. W. Liu, Aleksandra Wang, Jian'an Zhang, Jucheng Wang, Xinhong Sun, Jianzhong Chen, Fei Khalid, Syed Ghufran Jiang, Jun Zheng, Dingchang, Frontiers in Cardiovascular Medicine, "Extraction of coronary atherosclerotic plaques from computed tomography imaging: a review of recent methods," vol. 8, p. 597568, 2021.
[13] G. R. Sangiorgi, John A Severson, Arlen Edwards, William D Gregoire, Jean Fitzpatrick, Lorraine A Schwartz, Robert S, Journal of the American College of Cardiology, "Arterial calcification and not lumen stenosis is highly correlated with atherosclerotic plaque burden in humans: a histologic study of 723 coronary artery segments using nondecalcifying methodology," vol. 31, no. 1, pp. 126-133, 1998.
[14] M. N. Ghasemi, David R Lally, Caitriona, Journal of the Mechanical Behavior of Biomedical Materials, "Assessment of mechanical indicators of carotid plaque vulnerability: Geometrical curvature metric, plaque stresses and damage in tissue fibres," vol. 103, p. 103573, 2020.
[15] J. F. Zhao, Qianjin, IEEE Journal of Biomedical Health Informatics, "Automatic aortic dissection centerline extraction via morphology-guided CRN tracker," vol. 25, no. 9, pp. 3473-3485, 2021.
[16] M. H. Kobayashi, Katsuyuki Nemoto, Youkou Takagi, Shu Shojima, Masaaki Hayakawa, Motoharu Yamada, Shigeki Oshima, Marie, Computerized Medical Imaging Graphics, "A penalized spline fitting method to optimize geometric parameters of arterial centerlines extracted from medical images," vol. 84, p. 101746, 2020.
[17] M.-Y. S. Eun, Ha-Na Choi, Jong-Un Cho, Hwan-Ho Kim, Hyung Jun Chung, Jong-Won Song, Tae-Jin Jung, Jin-Man Bang, Oh-Young Kim, Gyeong-Moon, Scientific Reports, "Global intracranial arterial tortuosity is associated with intracranial atherosclerotic burden," vol. 14, no. 1, p. 11318, 2024.
[18] L. G. Aging Biomarker Consortium Zhang, Jun Liu, Yuehong Sun, Shimin Liu, Baohua Yang, Qi Tao, Jun Tian, Xiao-Li Pu, Jun, Life Medicine, "A framework of biomarkers for vascular aging: a consensus statement by the Aging Biomarker Consortium," vol. 2, no. 4, p. lnad033, 2023.
[19] K. M. K. M. S. W. Squillacote, vtk.js - VTK for the Web, 2017, https://kitware.github.io/vtk-js/.
[20] Y. T. Yan, Tengfei Zhao, Lijian Zhou, Yuchen Wang, Weihang, "Understanding the performance of webassembly applications," in *Proceedings of the 21st ACM Internet Measurement Conference*, 2021, pp. 533-549.
[21] M. A. AboArab, Potsika, Vassiliki T, Skalski, Andrzej, Stanuch, Maciej, Gkois, George, M. Koncar Igor, David, and A. Theodorou, Vagena, Sylvia, Sigala, Fragiska, Dimitrios I. Fotiadis, "DECODE-3DViz: Efficient WebGL-Based High-Fidelity Visualization of Large-Scale Images using Level of Detail and Data Chunk Streaming," *Journal of Imaging Informatics in Medicine,* pp. 1-19, 2025.
[22] J. T. Xu, Gaspard Chabat, Timothee McCormick, Matthew Li, Forrest Birdsong, Tom Martin, Ken Lee, Yueh Aylward, Stephen, Computer Methods in Biomechanics Biomedical Engineering: Imaging Visualization, "Interactive, in-browser cinematic volume rendering of medical images," vol. 11, no. 4, pp. 1019-1026, 2023.
[23] G. M. I. D. V. I. Viola and K. G. van der Walt, " Kitware Inc. Available: https://github.com/Kitware/glance.